Automatic Expert Selection for Multi-Scenario and Multi-Task Search

Xinyu Zou
zouxinyu@whu.edu.cn
School of Cyber Science and
Engineering, Wuhan University
China

Zhi Hu
tuopu.hz@antgroup.com
Ant Group
China

Yiming Zhao
desert.zym@antgroup.com
Ant Group
China

Xuchu Ding
dingxuchu.dxc@antgroup.com
Ant Group
China

Zhongyi Liu
zhongyi.lzy@antgroup.com
Ant Group
China

Chenliang Li[†]
cllee@whu.edu.cn
Key Laboratory of Aerospace
Information Security and Trusted
Computing, Ministry of Education,
School of Cyber Science and
Engineering, Wuhan University
China

Aixin Sun
axsun@ntu.edu.sg
Nanyang Technological University
Singapore

ABSTRACT

Multi-scenario learning (MSL) enables a service provider to cater for users' fine-grained demands by separating services for different user sectors, *e.g.,* by user's geographical region. Under each scenario there is a need to optimize multiple task-specific targets *e.g.,* click through rate and conversion rate, known as multi-task learning (MTL). Recent solutions for MSL and MTL are mostly based on the multi-gate mixture-of-experts (MMoE) architecture. MMoE structure is typically static and its design requires domain-specific knowledge, making it less effective in handling both MSL and MTL. In this paper, we propose a novel **A**utomatic **E**xpert **S**election framework for **M**ulti-scenario and **M**ulti-task search, named $AESM^2$. $AESM^2$ integrates both MSL and MTL into a unified framework with an automatic structure learning. Specifically, $AESM^2$ stacks multi-task layers over multi-scenario layers. This hierarchical design enables us to flexibly establish intrinsic connections between different scenarios, and at the same time also supports high-level feature extraction for different tasks. At each multi-scenario/multi-task layer, a novel expert selection algorithm is proposed to automatically identify scenario-/task-specific and shared experts for each input. Experiments over two real-world large-scale datasets demonstrate the effectiveness of $AESM^2$ over a battery of strong baselines. Online A/B test also shows substantial performance gain on multiple metrics. Currently, $AESM^2$ has been deployed online for serving major traffic.

CCS CONCEPTS

• **Information systems → Retrieval models and ranking**.

KEYWORDS

Multi-Task Learning, Multi-Scenario Learning, Search and Ranking

1 INTRODUCTION

To better serve users, many industrial searching systems start to split business into different scenarios by user sectors, item categories and traffic channels. For example, users may come to a search service through both PC browser and a mobile app, or through a home page or the specific vertical page. The things would become more complex such that fine-grained scenarios are organized as a hierarchical structure. Figure 1 shows such a prevalent situation that either brand and category based search can be accessed through home page and vertical page respectively. Although the same search service can be deployed at the back end, the combination of vertical page and brand based search certainly indicates a more focused demand while home page and category based search is more useful for general exploration.
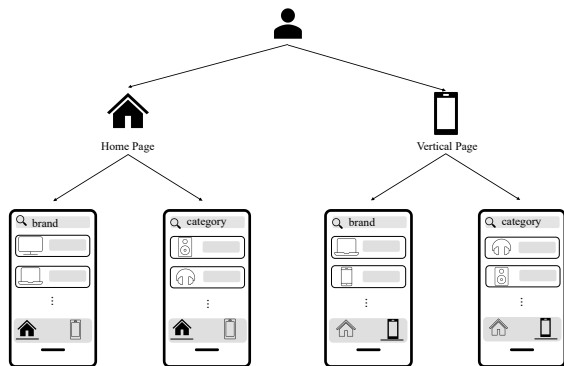
Figure 1: An example of a hierarchical structure of multiple fine-grained scenarios.

Naturally, many of these scenarios share some useful information towards user's intent, such as user profile, item features, and even the same queries. Apparently, searching systems can be enriched through information sharing across relevant scenarios with a Multi-scenario learning (MSL) setting, as shown in Figure 2(a). Under each scenario, user satisfaction and engagement are often quantified by different objectives, *e.g.,* Click-Though Rate (CTR) and Conversion Rate (CVR). Therefore, a Multi-task learning (MTL) setting could also be applied to leverage the intrinsic correlation between different tasks, as shown in Figure 2(b).

Recently, significant efforts have been devoted to devise different MSL and MTL solutions [1, 8, 11–13, 15, 16, 19, 20]. These solutions mainly exploit the multi-gate mixture-of-experts (MMOE) architecture to distill scenario-/task-specific information as well as the shared information among scenarios and tasks. To support efficient information sharing and alleviate the negative transfer [21], these solutions mainly resort to domain knowledge to design specific expert structure. For example, for MSL, STAR [19] proposes a star topology with a shared center and scenario-specific experts. TreeMS [15] chooses to model different E-Commerce scenarios with a tree structure. For MTL, PLE [20] handcrafts explicit separation between the task-specific and task-shared experts, for video and product recommendations. Note that these strategies require strong domain expertise to optimize the network structure. Nevertheless, the resultant structures are globally static across different scenarios, tasks, and inputs.

It is now becoming a business need to optimize a bunch of tasks across different scenarios, as shown in Figure 2(c). A straightforward solution is to deploy different MSL models for different tasks. On the one hand, this simple strategy will sacrifice the intrinsic correlations between the tasks that are validated to be beneficial in existing MSL solutions. On the other hand, optimizing the network structure for each task on the basis of MSL requires further expertise, leading to significant increase in maintenance cost. The same story can be told by reversing this order. Here, we are particularly interested in developing a unified framework that could realize both MSL and MTL requirements, and alleviate the above problems.

To this end, in this paper, we propose a novel **A**utomatic **E**xpert **S**election framework for **M**ulti-scenario and **M**ulti-task search, named AESM^2. To the best of our knowledge, this is the first work
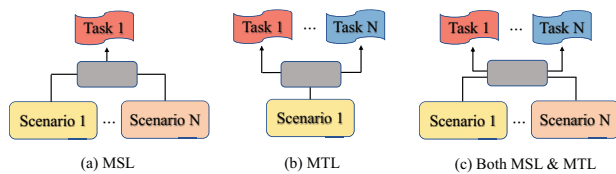

(a) MSL   (b) MTL   (c) Both MSL & MTL

Figure 2: Comparison of MSL, MTL, and MSL&MTL.

to tackle both MSL and MTL problems simultaneously within a unified ranking framework. AESM^2 is a flexible hierarchical structure where the multi-task layers are stacked over the multi-scenario layers. This hierarchical design bears two unique merits: 1) we can model the complex relations between different scenarios for more efficient information sharing. In a business setting, many scenarios can be organized as a hierarchical structure in nature. The hierarchical modeling of business logic further enhances efficiency of information sharing. Moreover, this hierarchical structure leads to significant reduction in computational cost (ref. Section 3.3); 2) we can make full use of intrinsic correlations among different tasks without deploying the different MSL design under each task, and vice versa. Again, this leads to large saving of maintenance cost.

Another core novelty in AESM^2 is a general expert selection algorithm for automatically extracting scenario/task-specific and the shared information, in each multi-scenario and multi-task layer. In detail, the selection process leverages scenario/task correlations and is anchored on the sparsification of multi-gate mixture-of-experts structure. We emphasize that expert selection is performed for each instance, so as to achieve an adaptive structure learning. We also devise an auxiliary loss function to guide the training of this selection process.

We perform extensive experiments on two real-world datasets, named AliPay and AliExpress, with different characteristics. Experimental results show that AESM^2 achieves substantial improvements over state-of-the-art models and possible technical alternatives. The online experiments also verify the superiority of our proposed AESM^2. To summarize, we make the following contributions in this paper:

- We introduce a novel automatic expert selection framework for multi-scenario and multi-task search. To the best of our knowledge, AESM^2 is the first work to enable both MSL and MTL simultaneously under a unified ranking framework.
- We devise a flexible and efficient hierarchical structure in AESM^2 to accommodate complex relations underlying different scenarios. Moreover, an expert selection algorithm is proposed to support adaptive structure learning, such that task-specific and shared information can be better harnessed in instance level. To guide the selection process, we further introduce an auxiliary loss to enhance model training.
- We conduct extensive experiments on two real-world large-scale searching datasets. Both offline and online experiments well demonstrate of the superiority of our proposed AESM^2. Currently, AESM^2 has been successfully deployed in AliPay to serve major online traffic.

2 RELATED WORK

In this section, we briefly review existing studies that are highly related to our work, specifically, multi-scenario learning, multi-task learning, and sparse experts network.

2.1 Multi-Scenario Learning

Multi-scenario learning aims at addressing the same task with a unified model under different scenarios, where the label spaces are of the same. STAR [19] tries to capture scenario correlations via star topology which consists of shared center parameters and scenario-specific parameters. Chen *et al.* utilize an auxiliary network to model shared knowledge separately [2]. ZEUS [3] focuses on numerous user behaviors across all scenarios, and performs self-supervised learning to improve ranking performance. Since MSL and MTL can be viewed in a unified perspective [26], other studies [8, 15] formulate this problem as a multi-task learning problem, and aim to optimize all scenarios with MMoE-like structure in an end-to-end way. Specifically, the core part of a multi-gate mixture-of-experts (MMoE) [11] is the gating mechanism that fuses the output of different parallel expert networks together. HMoE [8] represents each scenario with experts respectively, while TreeMs [15] represents scenarios as a semantic tree and utilize LSTM [4] to model scenario relations. However, all work discussed above are designed to adjust the basic MMoE structure to adapt a certain application.

2.2 Multi-Task Learning

Unlike MSL, multi-task learning focuses on modeling both intrinsic correlations (or information sharing) and specific knowledge across different tasks [11, 20, 23, 27], *e.g.,* click-though rate prediction & conversion rate prediction [8, 12] and credit risk forecasting & credit limits setting [9]. Hard parameter sharing [1] is the simplest model to learn intrinsic correlations through a shared bottom layer. To model more complex task correlations, recent work [13, 16] resort to MMoE to realize information sharing. However, they suffer from "Seesaw Phenomenon" [20] - the improvement of one task often leads to performance degeneration of some other tasks. Different from static linear combination, Ma *et al.* propose a flexible parameter sharing framework in multi-task setting [10]. Recently, PLE [20] adopts a progressive routing mechanism and separates experts into task-sharing and task-specific group in an explicit way, which alleviates the Seesaw Phenomenon in recommender systems.

2.3 Sparse Experts Network

Sparse experts network has been proven to be useful for improving computational efficiency and enhancing model performance [18, 22]. Various sparse policies have been studies where sparsity can be achieved through hard setting (*e.g.,* setting values to zeros and ones) like TopK [17, 24, 25] or in a more relaxed manner like gumbel-softmax [7, 14]. However, these work only considers sparse policy with regard to a single gate *i.e.,* MoE [5], which is not directly generalizable to multi-task and multi-scenario settings. To the best of our knowledge, our work is the first attempt that adapts sparse policy according to the task/scenario correlations on top of the basic MMoE structure.
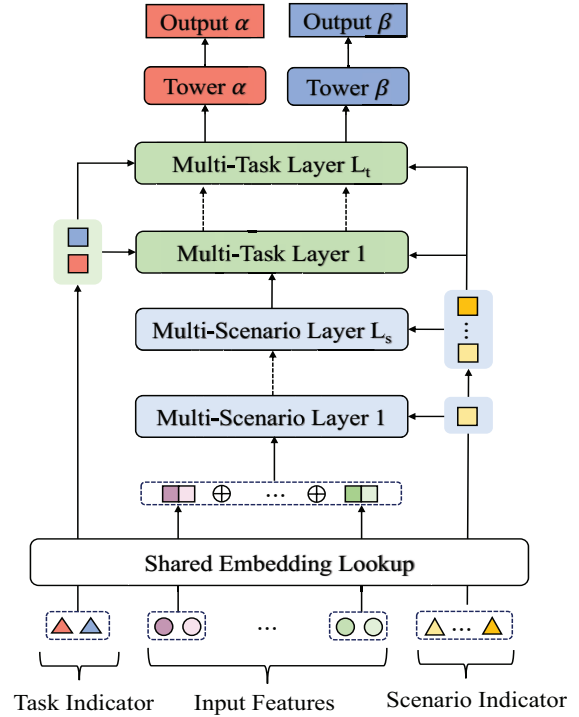
3 METHOD

Figure 3: The whole architecture of AESM[2].

In this section, we first formulate our research problem. Then, we introduce the basics of MMoE which serve as preliminary knowledge for our model. After detailing the components in our model, we present model optimization procedures.

3.1 Problem Formulation

In a searching system, users retrieve items through queries. In a multi-scenario & multi-task searching setting, users may be put under different scenarios for various tasks optimization. Formally, we have $\{S, \mathcal{T}, \mathcal{U}, \mathcal{I}, Q\}$. Here, S and $\mathcal{T}$ denote scenario set and task set respectively. User set $\mathcal{U}$ is composed of users from all scenarios: $\mathcal{U} = \mathcal{U}_1 \cup \mathcal{U}_2 \cdots \mathcal{U}_s$. The item set $\mathcal{I}$ and query set Q are defined in the same way. Given extensive features of users, items, and queries, our research problem is to optimize all tasks in $\mathcal{T}$ for every scenario. The goal is to learn a rating function $y_t(u, i, q)$ for each task: $\mathcal{U} \times \mathcal{I} \times Q \rightarrow \mathbb{R}^{|S| \times |\mathcal{T}|}$, where $y_t(u, i, q)$ is the ranking score of item i for user u who issues query q in the perspective of task t.

3.2 Basics of MMoE

The Multi-gate Mixture-of-Experts (MMoE) is designed to tackle multi-task problem, and is widely used in online platforms for ranking [8, 11] or addressing cold-start problem [15, 28]. We briefly review MMoE's network architecture, illustrated in Figure 4(a).

Suppose there are n experts and m tasks, and each expert is implemented as independent multi-layer perception, *i.e.,* $f_i(\cdot)$ and
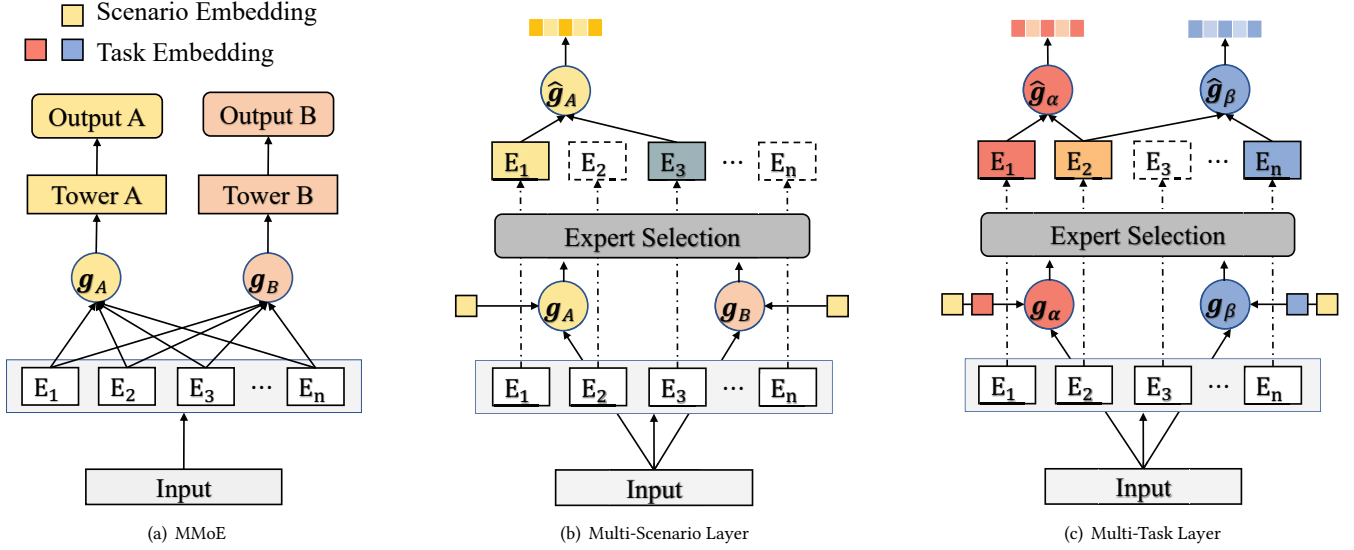
Figure 4: (a) Network structure of MMoE. (b) and (c) are illustrations of a single multi-scenario layer and a single multi-task layer, respectively in AESM^2

$1 \leq i \leq n$. A MMoE combines these experts together through a gating mechanism. Specifically, let $\mathbf{x}$ denote the input vector. The output of this MMoE module for a certain task t is shown as follows:

$$o_t(\mathbf{x}) = MMoE(\mathbf{x}, \mathbf{g}) = \sum_{i=1}^{n} \mathbf{g}_t[i] f_i(\mathbf{x}) \qquad (1)$$

$$f_i(\mathbf{x}) = \sigma(\mathbf{W}_i \mathbf{x}) \qquad (2)$$

where $\sigma(\cdot)$ is the nonlinear activation function, and $\mathbf{g}_t \in \mathbb{R}^n$ denotes gating scalar vector. Here, $\mathbf{g}_t[i]$ indicates the importance score for i-th expert, which is calculated as follows:

$$\mathbf{g} = \mathbf{W}_t \mathbf{x} \qquad (3)$$

$$\mathbf{g}_t = softmax(\mathbf{g}) \qquad (4)$$

where $\mathbf{W}_t$ is a learnable parameter of gating mechanism for task t.

3.3 The Proposed Model

Our model AESM^2 is illustrated in Figure 3. AESM^2 treats multi-scenario and multi-task in a similar way and adopts a hierarchical architecture to couple them into a unified framework. Different from optimizing a static structure, AESM^2 leverages a general and flexible architecture for selecting scenario/task-specific and scenario/task-shared experts automatically. In the following, we first introduce the shared embedding layer in AESM^2. For simplification, we detail a simple model with only a single multi-scenario layer (Figure 4(b)) and a single multi-task layer (Figure 4(c)). Lastly, we discuss the extension in a multi-layer setting.

Shared Embedding Layer. The shared embedding layer is devised to cast the raw categorical and numerical features into continuous embeddings. Supposed there are v groups of features, such as user group (*e.g.*, age, gender), item group (*e.g.*, price, brand), and query

group (*e.g.*, query frequency). For a given instance, we first transform numerical features into categorical types, and then encode each categorical feature to one-hot vector. Let user group be the first group, we project these one-hot vectors into corresponding embeddings and form the group embedding $\mathbf{x}_1$ as follows:

$$\mathbf{x}_1 = \left[\mathbf{W}_1^u \mathbf{x}_1^u, \mathbf{W}_2^u \mathbf{x}_2^u, \ldots, \mathbf{W}_{n_u}^u \mathbf{x}_{n_u}^u\right] \qquad (5)$$

where n_u is the number of features in user group, $[\cdot, \cdot]$ refers to vector concatenation. The same applies to other groups. Then we concatenate embeddings of all groups together to form the feature vector $\mathbf{x}$ as the input to the subsequent components in AESM^2:

$$\mathbf{x} = [\mathbf{x}_1, \mathbf{x}_2, \cdots, \mathbf{x}_v] \qquad (6)$$

where $\mathbf{x} \in \mathbb{R}^d$ and d is dimension size.

Meanwhile, scenario embedding $\mathbf{s}$ that indicates the scenario of a given data record, and task embeddings $\mathbf{t}_1, \mathbf{t}_2, \cdots, \mathbf{t}_{|\mathcal{T}|}$ including all tasks, are generated from scenario or task ids respectively. $|\mathcal{T}|$ is the size of task set.

Multi-Scenario Layer. After the shared embedding layer, we feed $\mathbf{x}$ into the multi-scenario layer for expert selection, to get the corresponding output in terms of the selected experts. For simplicity, we only show the selecting process of one layer in Figure 4(b), multiple layers can be stacked together if needed.

Suppose there are n experts and m scenarios (*i.e.*, m gates) in a multi-scenario layer. We first utilize a linear transformation to calculate the gating scalar vector for each scenario as follows:

$$\mathbf{G} = [\mathbf{g}_1, \cdots, \mathbf{g}_m] \qquad (7)$$

$$\mathbf{g}_j = \mathbf{S}_j[\mathbf{x}, \mathbf{s}] + \boldsymbol{\eta}_j \qquad (8)$$

Here $\mathbf{g}_j[k]$ is the relevance score between the j-th scenario and the k-th expert with respect to the input instance ($\mathbf{g}_j \in \mathbb{R}^n$). $\mathbf{S}_j$ is a learnable parameter; $\mathbf{s}$ is the scenario embedding of the given data record; $\boldsymbol{\eta}_j$ is the Gaussian noise whose scale is positively

proportional to n (*i.e.*, $\|\boldsymbol{\eta}_j\| \propto n$); and $\mathbf{G} \in \mathbb{R}^{n \times m}$. The introduced gaussian noise will guide our model to explore search space for better expert selection.

Expert row vector $\mathbf{G}[k,:] = \big[\mathbf{G}[k,1], \cdots, \mathbf{G}[k,m]\big]$ is the key for expert selection. We assume that if $\mathbf{G}[k,j]$ gets relatively higher score than the other elements in $\mathbf{G}[k,:]$, the k-th expert is more likely classified into scenario-specific group of j-th scenario. If values in $\mathbf{G}[k,:]$ all get closer to each other relatively, then the k-th expert may contain shared information among all scenarios. Hence, we firstly perform a row-wise softmax operation over matrix $\mathbf{G}$ as follows:

$$\tilde{\mathbf{G}} = softmax(\mathbf{G}) \tag{9}$$

Then, for the j-th scenario, we form an one-hot scenario indicator vector $\mathbf{p}_j \in \mathbb{R}^m$ where only the j-th element is 1 (*e.g.*, $[1, \cdots, 0]$ for the first scenario). As aforementioned, the likelihood of the k-th expert being a scenario-specific group for j-th scenario can be measured by the similarity between $\mathbf{p}_j$ and $\tilde{\mathbf{G}}[k,:]$.

Similarly, we also introduce an uniform vector $\mathbf{q}_j \in \mathbb{R}^m$ for j-th scenario: $\mathbf{q}_j = [1/m, \cdots, 1/m]$. The likelihood of k-th expert being a scenario-shared group for j-th scenario can be measured by the similarity between $\mathbf{q}_j$ and $\tilde{\mathbf{G}}[k,:]$. Formally, the selection process for generating scenario-specific and scenario-shared expert indices is described as follows:

$$\mathcal{E}_{sp} = TopK(h_1^p, \cdots, h_n^p) \tag{10}$$

$$h_k^p = -KL(\mathbf{p}_j, \tilde{\mathbf{G}}[k,:]) \tag{11}$$

$$\mathcal{E}_{sh} = TopK(h_1^q, \cdots, h_n^q) \tag{12}$$

$$h_k^q = -KL(\mathbf{q}_j, \tilde{\mathbf{G}}[k,:]) \tag{13}$$

where $\mathcal{E}_{sp}$ and $\mathcal{E}_{sh}$ respectively refer to the scenario-specific and scenario-shared expert index set for j-th scenario. Function $TopK(\cdot)$ is the argument operation that returns the indices of top-K values, and $KL(\cdot)$ calculates the Kullback-Leibler divergence where a lower divergence score means a higher similarity of the two distributions.

With $\mathcal{E}_{sp}$ and $\mathcal{E}_{sh}$, we update the gating scalar vector $\mathbf{g}_j$ to accomplish sparse experts network:

$$\hat{\mathbf{g}}_j[k] = \begin{cases} \mathbf{g}_j[k], & if \quad k \in \mathcal{E}_{sh} \cup \mathcal{E}_{sp} \\ -\infty, & else \end{cases} \tag{14}$$

Following Equation 1, the output of this scenario layer can be derived with the updated gating scalar matrix $\hat{\mathbf{g}}_j$ and the outputs of n experts via a standard MMoE module:

$$\mathbf{z}_j = ScenarioLayer(\mathbf{x}, \mathbf{s}_j) = MMoE(\mathbf{x}, \hat{\mathbf{g}}_j) \tag{15}$$

where $\mathbf{z}_j$ is the output for j-th scenario.

Multi-Task Layer. Given the output $\mathbf{z}_j$ from the above multi-scenario layer, we also utilize the same selection process to achieve multi-task learning. Assuming there are n experts and t tasks in the multi-task layer, we calculate the gating scalar vector $\mathbf{g}_k$ for k-th task as follows:

$$\mathbf{g}_k = \mathbf{T}_k[\mathbf{x}, \mathbf{s}, \mathbf{t}_k] + \boldsymbol{\eta}_k \tag{16}$$

where $\mathbf{T}_k$ is a learnable parameter, $\mathbf{t}_k$ denotes the embedding of k-th task, $\boldsymbol{\eta}_t$ is the Gaussian noise similar to Equation 8. By forming the one-hot task indicator vector and uniform vector for each task, we select the task-specific experts for each task and task-shared
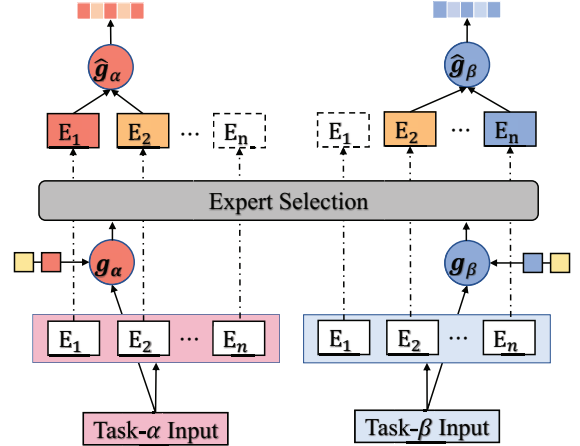

Figure 5: The network structure of multi-task layers with different task inputs.

experts respectively, following Equations 9-14. The resultant gating scalar vector $\hat{\mathbf{g}}_k$ is used to derive the output of each task via a MMoE module:

$$\mathbf{z}_k = TaskLayer(\mathbf{z}_j, \mathbf{t}_k) = MMoE(\mathbf{z}_j, \hat{\mathbf{g}}_k) \tag{17}$$

Then, we feed the output $\mathbf{z}_k$ into a tower of MLP to generate the prediction for k-th task:

$$\hat{y}_k = \sigma(MLP(\mathbf{z}_k)) \tag{18}$$

where $\hat{y}_k$ is the prediction for k-th task.

Multi-Layer Extension. In real-world applications, a scenario could be complex and exhibits a hierarchical structure in nature [15, 24]. For example, two search services α_1 and α_2 for two different domains (*e.g.*, search by brand, and search by feature) can be accessed through two different channels β_1 and β_2 (*e.g.*, home page and vertical page shown in Figure 1). These two channels may hold some unique characteristics against each other, and could be considered as two parent scenarios. Hence, we can form four fine-grained scenarios: $\beta_1 \rightarrow \alpha_1$, $\beta_1 \rightarrow \alpha_2$, $\beta_2 \rightarrow \alpha_1$ and $\beta_2 \rightarrow \alpha_2$.

Our proposed AESM^2 can be easily extended to accommodate this complex situation by stacking multiple multi-scenario layers together (each with a different parameter set). As shown in Figure 3, we can stack multiple multi-scenario layers to reach more complex multi-scenario modeling. Given there are L_s multi-scenario layers, the only modification in l-th layer is to update the scenario embedding $\mathbf{s}$ in Equation 8 as $[\mathbf{s}_1, \cdots, \mathbf{s}_l]$, where s_i is the embedding of the specified scenario in i-th layer, $1 < l \le L_s$. In fact, we can model $n_1 \times n_2 \cdots n_{L_s}$ fine-grained scenarios. Note that when if a standard MMoE architecture is used, we need the same number of experts. In this sense, we can significantly reduce computation cost because $\sum_{i=1}^{L_s} n_i \ll n_1 \times n_2 \cdots n_{L_s}$.

As the design of AESM^2 is modular and flexibly, we can stack L_t multi-task layers together for higher-level feature extraction for each task (ref. Figure 5). However, things become slightly different because we have different input for each task after the first multi-task layer. To address this, we decide to share the same set of experts in each of the later multi-task layers, and perform expert

Table 1: Statistics of AliPay dataset. *#impress*, *#clk*, and *#cv* are the numbers of impressions, clicks, conversions respectively. *all* is the merged data of all scenarios. *#impress%* represents the percentage of *#impress* in one scenario among all scenarios, similarly *#clk%*, and *#cv%*.

	ALL	HP&RI	HP&BS	VP&RI	VP&BS
#impress	96,612,494	12,543,990	27,930,226	49,919,544	6,218,734
#clk	26,519,344	3,554,662	650,338	21,833,316	481,028
#cv	1,664,640	310,917	25,495	1,311,422	16,806
#clk/#impress	27.45%	28.34%	2.33%	43.74%	7.74%
#cv/#impress	1.72%	2.48%	0.09%	2.63%	0.27%
#cv/#clk	6.28%	8.75%	3.92%	6.00%	3.49%
#impress%	100%	12.98%	28.91%	51.67%	6.44%
#clk%	100%	13.40%	2.45%	82.33%	1.82%
#cv%	100%	18.68%	1.53%	78.78%	1.00%

Table 2: Statistics of AliExpress dataset.

	ALL	NL	FR	ES	US
#impress	103,814,836	17,717,195	27,035,601	31,669,427	27,392,613
#clk	2,215,494	381,078	542,753	842,055	449,608
#cv	58,171	13,815	14,430	19,096	10,830
#clk/#impress	2.13%	2.15%	2.00%	2.66%	1.64%
#cv/#impress	0.06%	0.08%	0.05%	0.06%	0.04%
#cv/#clk	2.63%	3.63%	2.66%	2.27%	2.41%
#impress%	100%	17.07%	26.04%	30.51%	26.39%
#clk%	100%	17.20%	24.50%	38.01%	20.29%
#cv%	100%	23.75%	24.81%	32.83%	18.62%

selection with different inputs. Following Equations 16 and 17, we derive the output for l-th multi-task layer by taking the output from the preceding layer $\mathbf{z}_k^{l-1}$ as input, where $l > 1$. Also, the scenario embedding $\mathbf{s}_j$ used in Equation 16 keeps the same as $[\mathbf{s}_1, \cdots, \mathbf{s}_{L_s}]$ for all multi-task layers. Figure 5 illustrates the architecture of such a multi-task layer. The prediction is made in terms of the output of the last multi-task layer by following Equation 18.

$$\mathcal{L}_k = -y_j^k \log\left(\hat{y}_j^k\right) - \left(1 - y_j^k\right) \log\left(1 - \hat{y}_j^k\right) \tag{19}$$

where y_j^k is the ground-truth label of j-th instance on k-th task, *e.g.*, a click (*i.e.*, *CTR*) or a conversion (*i.e.*, *CTCVR*), and $\mathcal{L}_k$ is the prediction loss for k-th task.

3.4 Model Optimization

Since the prediction for search task can be formulated as a probability prediction problem, we choose sigmoid function as the activation in Equation 18. Accordingly, we adopt the widely used Cross-Entropy loss for j-th instance as follows:

We also propose an auxiliary loss $\mathcal{L}_{aux}$ to guide the scenario/task expert selection. Specifically, for L_s multi-scenario layers, we aim to enhance the expert selection decision during the training process

as follows:

$$\mathcal{L}_{sp}^s = \sum_{l=1}^{L_s} \sum_{k \in \mathcal{E}_{sp}} KL(\mathbf{p}_j, \tilde{\mathbf{G}}^l[k,:]) \tag{20}$$

where $\tilde{\mathbf{G}}^l[k,:]$ is the output of Equation 9 in l-th multi-scenario layer. Similarly, we can enhance the expert selection decision for L_t multi-task layers with loss $\mathcal{L}_{sp}^t$. The two auxiliary losses are summed as $\mathcal{L}_{sp} = \mathcal{L}_{sp}^s + \mathcal{L}_{sp}^t$. The same goes for the expert selection in the scenario/task-shared side, denoted by $\mathcal{L}_{sh}$. The final auxiliary loss $\mathcal{L}_{aux}$ is then defined as follows:

$$\mathcal{L}_{aux} = \lambda_{sp} \mathcal{L}_{sp} + \lambda_{sh} \mathcal{L}_{sh} \tag{21}$$

where λ_{sp} and λ_{sh} are hyper-parameters to tune. That is, $\mathcal{L}_{sp}$ enhances the selecting process by guiding the gating scalar distribution of a specific experts network get close to the assumed specific distribution $\mathbf{p}_j$. The same goes for $\mathcal{L}_{sh}$. Finally, we get the overall loss function for our model:

$$\mathcal{L} = \sum_{k=1}^{t} \lambda_k \mathcal{L}_k + \mathcal{L}_{aux} + \gamma \|\Theta\|_2^2 \tag{22}$$

where λ_k and γ are hyper-parameters, and $\|\Theta\|_2$ denotes $L2$ regularization over model parameters. Adam [6] is chosen as the optimizer to perform gradient backpropagation for model optimization.

Table 3: Performance comparison in AliPay dataset. The best results are in boldface and second best underlined. Symbol * indicates that difference to the best baseline is statistically significant at 0.05 level.

Model	HP&RI		HP&BS		VP&RI		VP&BS		ALL	
	auc_ctr	auc_ctcvr	auc_ctr	auc_ctcvr	auc_ctr	auc_ctcvr	auc_ctr	auc_ctcvr	auc_ctr	auc_ctcvr
Hard Sharing	90.89	90.95	77.14	81.60	86.27	85.56	69.51	75.64	90.34	89.15
Parallel DNN	91.22	91.55	77.03	81.37	86.34	85.79	70.57	76.46	90.62	89.60
Cross-Stitch	91.12	91.59	77.06	81.82	86.39	86.08	70.86	76.79	90.63	89.82
STAR	90.62	91.66	74.04	81.86	85.66	86.34	69.29	77.13	89.98	90.00
MMoE	91.06	91.71	77.54	82.31	86.36	86.36	69.94	77.18	90.62	90.03
HMoE	89.05	89.54	75.61	79.68	85.32	85.24	65.52	70.56	89.58	88.72
PLE	91.11	91.76	77.05	81.93	86.35	86.47	70.90	77.03	90.63	90.10
AESM^2	91.49*	92.21*	78.22*	82.98*	86.73*	86.91*	72.13*	78.33*	90.86*	90.42*

4 EXPERIMENTS

In this section, we evaluate our proposed AESM^2 against a series of state-of-the-art baselines. Extensive experiments on two real-world large-scale searching datasets with both multi-scenario and multi-task settings demonstrate the effectiveness of our model, which is further confirmed by the online A/B test across multiple business metrics. At last, we provide in-depth analysis about model components.

4.1 Experimental Setup

Datasets. We collect **AliPay** dataset sampled from anonymous user daily search logs on AliPay mobile application[1] from Nov. 15 to Nov. 30 2021. In AliPay dataset, there exists a hierarchical structure among scenarios: *channel → domain*. There are two channels: home page (HP) and vertical page (VP), and two domains: regular items (RI) and best sellers (BS). As the result, we have four scenarios listed in Table 1, *e.g.*, HP→ RI, VP→RI. We split the data by date for model training and evaluation: data in Nov. 15-Nov. 28 for training, Nov. 29, 2021 for validation, and Nov. 30, 2021 for testing. Also, there are two tasks for this dataset: click ratio (CTR) and conversion ratio (CTCVR).

Moreover, we also conduct experiments on a public E-Commerce dataset **AliExpress**[2]. This dataset also includes multi-scenarios (split by user nationality) and multi-task (CTR and CTCVR) settings. Here, we choose four scenarios: *NL*, *FR*, *ES*, and *US*[3] on AliExpress dataset. Because the original dataset only contains training set and testing set, we randomly sample 50% of the original testing data as validation set.

The detailed statistics of the two datasets are reported in Table 1 and 2. Observe that data distribution in both datasets is imbalanced. For example, the number of impressions in VP→BS scenario only accounts for 6.44% on all scenarios, and majority clicks happen in scenario VP→RI, which accounts for 82.33% instead.

Baselines. We compare AESM^2 with two categories of baselines: (1) *gate-aware models* which use gating mechanism to tackle multi scenario or multi-task problems, including MMoE [11], HMoE [8], and PLE [20]. (2) *gate-free models* including Hard Sharing [1], Parallel DNN, Cross-Stitch [13] and STAR [19]. Baselines in the latter category leverage other solutions to model correlations across scenarios or tasks.

- **Hard Sharing** [1] is a simple but widely-used model, to encode common knowledge via a shared bottom layer.
- **Parallel DNN** is adapted from basic DNN to fit multiple scenarios or tasks, where parallel transformation is added for each task/scenario.
- **Cross-Stitch** [13] combines multiple networks together via linear cross-stitch units to learn a task-specific representation.
- **MMoE** [11] exploits multi-gate mixture experts to model relationships among experts implicitly. The merged representations from multiple gates can be transformed to multiple scenario/task prediction layers respectively.
- **HMoE** [8] extends MMoE to scenario-aware experts with gradient-cutting trick for encoding scenario correlation explicitly. HMoE leverages two models with separate parameters for optimizing CTR and CVR respectively.
- **STAR** [19] adopts star topology with a shared center network and scenario-specific network for CTR prediction task.
- **PLE** [20] is another state-of-art MMoE variant that separates experts into task-specific groups and task-shared groups for the purpose of avoiding negative transfer and seesaw phenomenon.

Metrics and Implementation[4]. Following ESMM [12], we optimize CTR and CVR in an entire space, *i.e.*, $CTCVR = CTR \times CVR$, where CTR and CVR are the output of CTR tower and CVR tower respectively. The well-known area under ROC curve (AUC) is adopted to evaluate both CTR and CTCVR performances. Data of all scenarios are merged together at input level, and performance under every single scenario as well as the merged all are compared.

Note that, none of baselines consider optimizing MSL&MTL problem simultaneously within one model. Hence, we extend their structure to adapt to our experiment setting. For example, for multi-scenario model STAR, we implement another star topology in task-level structure. For multi-task model PLE, we extend it with additional progressive layered extraction to tackle multi-scenario problem. In addition, all baselines are trained with merged scenarios

---

[1] https://global.alipay.com/platform/site/ihome
[2] https://tianchi.aliyun.com/dataset/dataDetail?dataId=74690
[3] The four scenarios indicate the users from Netherlands (NL), France (FR), Spain (ES) and United States (US).

[4] The code implementation is available at https://github.com/alipay/aes_msl_mtl.

Table 4: Performance comparison in AliExpress dataset. The best results are in boldface and second best underlined. Symbol * indicates that difference to the best baseline is statistically significant at 0.05 level.

Model	NL		FR		ES		US		ALL	
	auc_ctr	auc_ctcvr	auc_ctr	auc_ctcvr	auc_ctr	auc_ctcvr	auc_ctr	auc_ctcvr	auc_ctr	auc_ctcvr
Hard Sharing	70.70	81.49	70.89	81.41	70.57	83.89	69.71	79.36	70.59	81.56
Parallel DNN	71.11	84.17	70.96	84.91	70.60	85.91	69.17	79.38	70.38	83.98
Cross-Stitch	72.04	84.92	71.59	86.50	71.77	87.56	69.66	83.02	71.28	85.91
STAR	71.45	84.76	71.29	86.36	71.94	88.21	<u>70.03</u>	85.63	71.32	86.49
MMoE	71.77	84.87	71.45	86.18	72.16	87.75	69.83	84.87	71.42	86.15
HMoE	71.87	85.47	71.56	86.76	72.06	88.01	69.81	84.71	71.41	86.50
PLE	<u>71.91</u>	<u>85.60</u>	<u>71.60</u>	<u>86.95</u>	<u>72.31</u>	<u>88.53</u>	69.90	<u>86.18</u>	<u>71.56</u>	<u>87.11</u>
AESM^2	**72.60***	**86.38***	**72.41***	**88.08***	**72.95***	**89.49***	**70.88***	**87.74***	**72.30***	**88.12***

Table 5: AUC results (CTR) of transferring to different scenarios. The value of row i and column j means trained on *scenario i* and tested on *scenario j*

Train \ Test	HP&RI	HP&BS	VP&RI	VP&BS
HP&RI	90.61	58.68	76.34	58.46
HP&BS	54.25	77.92	53.28	63.52
VP&RI	86.87	52.78	85.85	55.96
VP&BS	59.61	64.91	60.52	70.43

data, and are then used to predict both CTR and CTCVR, the same as AESM^2. Experts in every MMoE-like models are implemented as a single-layer network. For fair comparison, we implement all models with same depth level, all MMoE variant models share the same number of activated experts during training. PLE and AESM^2 share the same size of specific/shared experts set (*i.e.,* 3 in AliPay and 10/3 for domain/task layer in AliExpress). The K value is set to 1 and 2/1 for them respectively.

Recall that, there are two channels and two domains in AliPay dataset before the specific tasks. we implement all models in a stacked way corresponding to the scenario hierarchy of the dataset.

4.2 Performance Comparison

Table 3 and 4 report performance of all models on AliPay and AliExpress datasets, respectively.

Results in both tables show that our proposed model AESM^2 consistently outperforms all baselines over all scenarios on all tasks. This result indicates that our model performs well in Multi-scenario&Multi-task settings and is able to adapt to different configurations of scenarios and tasks. Observe that our model gains significant improvement especially on hard scenarios, *e.g.,* VP&BS scenario of AliPay that suffers from the the highest data sparsity with only 6.44% impressions.

The results show a broader "SeeSaw Phenomenon" in Multi-scenario&Multi-task settings among baseline models. That is, multiple tasks could not be improved simultaneously compared to other models in one certain scenario. In other words, performance gain of one metric cannot be achieved consistently across other scenarios. For instance, when compared by CTR in AliPay, PLE performs
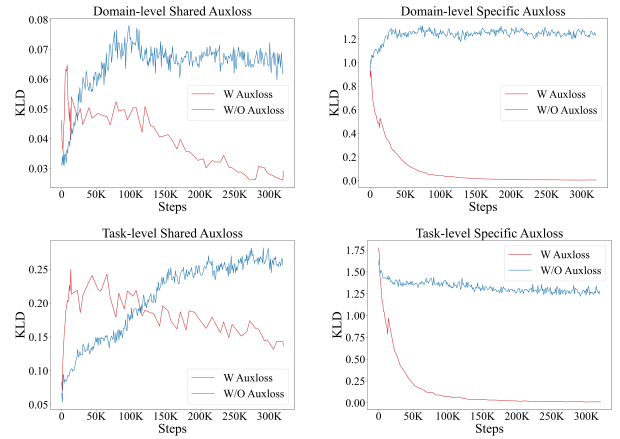

Figure 6: Kullback-Leibler divergence curves of both scenario and task levels on AliPay dataset. X-axis denotes training steps, y-axis is the summation of KL values between the assumed distribution and the selected row vector of gating matrix in Equation 20; lower y value means closer distance to the assumed distribution.

better than MMoE in VP&BS scenario but worse than MMoE in HP&BS scenario. When compared in the scenario of ES in AliExpress dataset, STAR outperforms HMoE on CTR but is poorer than HMoE on CTCVR. This observation is consistent with what has been previously reported in [19, 20]. However, AESM^2 does not demonstrate SeeSaw phenomenon, compared with other baselines.

Finally, HMoE performs the poorest, even worse than Hard Sharing on AliPay dataset across all scenarios and tasks, but better performance is observed on AliExpress. One possible reason is that the task layer is attached with deeper levels for AliPay (*channel $\rightarrow$ domain $\rightarrow$ task*) than AliExpress (*domain $\rightarrow$ task*). The capability of modeling scenario correlations for HMoE could be easily corrupted because of the gradient-cutting trick.

4.3 Analysis of Scenario Relationships

We conduct experiments to quantify scenario relationships in Ali-Pay dataset. Specifically, we train a single Multi-task model (ESMM) [12] for each scenario, and produce predictions for all scenarios during

Table 6: Performance comparison for AESM^2 and its two variants on AliPay dataset. noise: Gaussian noise η (ref. Equation 16); auxloss: auxiliary loss $\mathcal{L}_{aux}$ (ref. Equation 21)

Model	HP&RI		HP&BS		VP&RI		VP&BS		ALL	
	auc_ctr	auc_ctcvr	auc_ctr	auc_ctcvr	auc_ctr	auc_ctcvr	auc_ctr	auc_ctcvr	auc_ctr	auc_ctcvr
AESM^2 w/o (noise&auxloss)	91.30	91.91	77.92	82.63	86.48	86.44	71.72	77.41	90.71	90.02
AESM^2 w/o auxloss	91.32	91.95	78.14	82.69	86.59	86.61	71.86	77.68	90.80	90.28
AESM^2	91.49	92.21	78.22	82.98	86.73	86.91	72.18	78.33	90.86	90.42

Table 7: AUC results (CTCVR) of transfering to different scenarios.

Train \ Test	HP&RI	HP&BS	VP&RI	VP&BS
HP&RI	91.18	65.36	79.40	65.51
HP&BS	53.25	82.11	51.56	65.64
VP&RI	87.35	53.62	85.38	66.13
VP&BS	55.02	73.26	58.51	74.04

Table 8: The relative improvements on AliPay App with online A/B test. GMV refers to Gross Merchandise Volume.

Metric	CTR	CVR	CTCVR	GMV
Relative Improved	+0.10%	+2.61%	+2.51%	+7.21%

inference phase. The results of CTR and CTCVR on test set of each scenario are shown in Table 5 and 7 respectively.

It is intuitive that the best performance for a model is obtained by its own data. In other words, each scenario in AliPay dataset has its own pattern. Scenarios in a same domain type get closer than other scenarios by both CTR and CTCVR metrics. This result suggests that there exists inner similarities and differences among scenarios.

Compared with models trained in the multi-scenario&multi-task setting (ref. Table 3), all baselines suffer from negative transfer from different scenarios. For instance, their performance on HP&BS is inferior to the model trained on single scenario. However, our AESM^2 outperforms all single-scenario models across all scenarios, which implies that our model can make better use of scenario relationships and avoid negative transfer.

4.4 Ablation Study

To study the impact of each component, we come up with two variants of AESM^2: (i) without Gaussian noise & auxiliary loss, and (ii) without auxiliary loss, for ablation study. According to Table 6, the simplest variant gets worst performance on all tasks for all scenarios. Gaussian noise η (ref. Equation 16) works well in all scenarios. This implies that a reasonable fluctuation would enable more freedom to explore the expert selection space and achieve a more accurate structure.

As to the auxiliary loss $\mathcal{L}_{aux}$ (ref. Equation 21), it promotes the selecting procedure by guiding the gating scalar value of specific/shared experts network to get closer to the assumed specific/shared distribution. Table 6 shows that the performance across all the combinations of scenario and task degrade when removing

Table 9: The result of online A/B test in each single scenario.

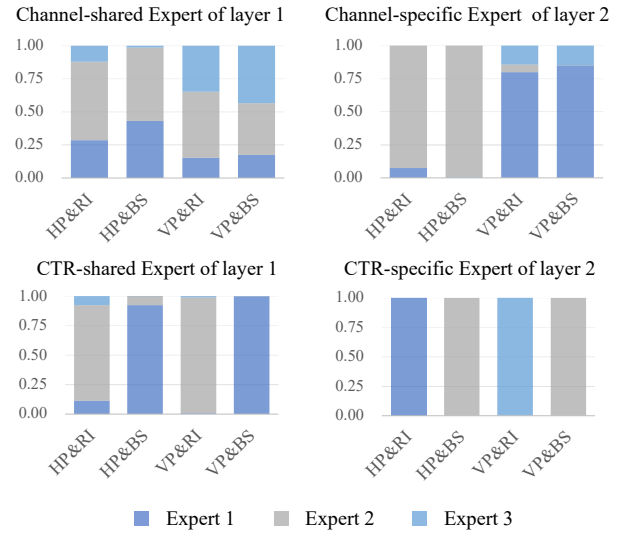| Scenario	CTCVR	GMV
HP&RI	+4.91%	+12.97%
HP&BS	+5.84%	+31.15%
VP&RI	+1.60%	+4.86%
VP&BS	+8.78%	+14.81%

Figure 7: Expert utilization rate for being grouped into specific or shared group in different layer.

$\mathcal{L}_{aux}$. We further plot the Kullback-Leibler divergence between the selected scenario/task distributions in the gating matrix and the assumed distribution (ref. Equation 20) in Figure 6. It is obvious to see that AESM^2 can produce sharper expert selection decisions by including $\mathcal{L}_{aux}$.

4.5 Visualization of Expert Utilization

We now investigate the expert utilization for both scenario/task-specific group and scenario/task-shared group respectively in AliPay dataset. For simplicity, every level (*i.e.,* channel, domain and task) contains two layers. Both specific expert set and shared expert set are configured to select only one expert. Figure 7 shows that in channel level, scenarios sharing the same type of channel have closer distributions. This indicates that our model can dynamically model complex patterns of shared information and disparity

across scenarios. On the contrast, PLE defines specific/shared experts in a static way. At task level, we observe each task almost selects one certain experts in specific/shared group, meaning that our model can also converge to PLE setting. These observations suggest that AESM^2 is a more general model which can adapt to different structure across scenarios/tasks.

4.6 Online A/B Test

Currently, AESM^2 is deployed on AliPay search system with the objective of maximizing CTCVR. We conduct a two-weeks' online A/B test against the latest previously deployed search system on AliPay. Table 8 shows the average relative improvements obtained by our model, suggesting AESM^2 promotes online industrial applications on all metrics.

We further investigate the performance on single scenarios. From Table 9, we can observe that both CTCVR and GMV get considerable improvement on each single scenario. The different amounts of improvement are dependent on the scale of each scenario (ref. Table 1).

5 CONCLUSION

A large-scale search system consists of a series of fine-grained scenarios that share some inherent connections and bear distinct characteristics. The need to optimize diverse tasks across different scenarios in a cost-effective fashion is becoming increasingly urgent. In this paper, we propose a unified framework of integrating both MSL and MTL under an adaptive learning paradigm. Both offline and online evaluations well validate the superiority of our proposed AESM^2 in terms of both search accuracy and business values. Also, AESM^2 has been successfully deployed in the AliPay search platform for handling major traffic. We plan to extend the proposed AESM^2 to support search explainability in the near future.

REFERENCES

[1] Rich Caruana. 1997. Multitask learning. *Machine learning* 28, 1 (1997), 41–75.
[2] Yuting Chen, Yanshi Wang, Yabo Ni, An-Xiang Zeng, and Lanfen Lin. 2020. Scenario-aware and Mutual-based approach for Multi-scenario Recommendation in E-Commerce. In *Proceedings of the International Conference on Data Mining Workshops (ICDMW)*. IEEE, 127–135.
[3] Yulong Gu, Wentian Bao, Dan Ou, Xiang Li, Baoliang Cui, Biyu Ma, Haikuan Huang, Qingwen Liu, and Xiaoyi Zeng. 2021. Self-Supervised Learning on Users' Spontaneous Behaviors for Multi-Scenario Ranking in E-commerce. In *Proceedings of the 30th ACM International Conference on Information & Knowledge Management*. 3828–3837.
[4] Sepp Hochreiter and Jürgen Schmidhuber. 1997. Long short-term memory. *Neural computation* 9, 8 (1997), 1735–1780.
[5] Robert A Jacobs, Michael I Jordan, Steven J Nowlan, and Geoffrey E Hinton. 1991. Adaptive mixtures of local experts. *Neural computation* 3, 1 (1991), 79–87.
[6] Diederik P Kingma and Jimmy Ba. 2014. Adam: A method for stochastic optimization. *arXiv preprint arXiv:1412.6980* (2014).
[7] Wouter Kool, Chris J Maddison, and Andriy Mnih. 2021. Unbiased Gradient Estimation with Balanced Assignments for Mixtures of Experts. *arXiv preprint arXiv:2109.11817* (2021).

[8] Pengcheng Li, Runze Li, Qing Da, An-Xiang Zeng, and Lijun Zhang. 2020. Improving Multi-Scenario Learning to Rank in E-commerce by Exploiting Task Relationships in the Label Space. In *Proceedings of the 29th ACM International Conference on Information & Knowledge Management*. 2605–2612.
[9] Ting Liang, Guanxiong Zeng, Qiwei Zhong, Jianfeng Chi, Jinghua Feng, Xiang Ao, and Jiayu Tang. 2021. Credit Risk and Limits Forecasting in E-Commerce Consumer Lending Service via Multi-view-aware Mixture-of-experts Nets. In *Proceedings of the 14th ACM International Conference on Web Search and Data Mining*. 229–237.
[10] Jiaqi Ma, Zhe Zhao, Jilin Chen, Ang Li, Lichan Hong, and Ed H Chi. 2019. Snr: Sub-network routing for flexible parameter sharing in multi-task learning. In *Proceedings of the AAAI Conference on Artificial Intelligence*, Vol. 33. 216–223.
[11] Jiaqi Ma, Zhe Zhao, Xinyang Yi, Jilin Chen, Lichan Hong, and Ed H Chi. 2018. Modeling task relationships in multi-task learning with multi-gate mixture-of-experts. In *Proceedings of the 24th ACM SIGKDD International Conference on Knowledge Discovery & Data Mining*. 1930–1939.
[12] Xiao Ma, Liqin Zhao, Guan Huang, Zhi Wang, Zelin Hu, Xiaoqiang Zhu, and Kun Gai. 2018. Entire space multi-task model: An effective approach for estimating post-click conversion rate. In *Proceedings of the 41st International ACM SIGIR Conference on Research & Development in Information Retrieval*. 1137–1140.
[13] Ishan Misra, Abhinav Shrivastava, Abhinav Gupta, and Martial Hebert. 2016. Cross-stitch networks for multi-task learning. In *Proceedings of the IEEE conference on computer vision and pattern recognition*. 3994–4003.
[14] Xiaonan Nie, Shijie Cao, Xupeng Miao, Lingxiao Ma, Jilong Xue, Youshan Miao, Zichao Yang, Zhi Yang, and Bin Cui. 2021. Dense-to-Sparse Gate for Mixture-of-Experts. *arXiv preprint arXiv:2112.14397* (2021).
[15] Xichuan Niu, Bofang Li, Chenliang Li, Jun Tan, Rong Xiao, and Hongbo Deng. 2021. Heterogeneous Graph Augmented Multi-Scenario Sharing Recommendation with Tree-Guided Expert Networks. In *Proceedings of the 14th ACM International Conference on Web Search and Data Mining*. 1038–1046.
[16] Sebastian Ruder, Joachim Bingel, Isabelle Augenstein, and Anders Søgaard. 2017. Sluice networks: Learning what to share between loosely related tasks. *arXiv preprint arXiv:1705.08142* 2 (2017).
[17] Carlos Riquelme Ruiz, Joan Puigcerver, Basil Mustafa, Maxim Neumann, Rodolphe Jenatton, André Susano Pinto, Daniel Keysers, and Neil Houlsby. 2021. Scaling Vision with Sparse Mixture of Experts. *arXiv preprint arXiv:2106.05974* (2021).
[18] Noam Shazeer, Azalia Mirhoseini, Krzysztof Maziarz, Andy Davis, Quoc Le, Geoffrey Hinton, and Jeff Dean. 2017. Outrageously large neural networks: The sparsely-gated mixture-of-experts layer. *arXiv preprint arXiv:1701.06538* (2017).
[19] Xiang-Rong Sheng, Liqin Zhao, Guorui Zhou, Xinyao Ding, Binding Dai, Qiang Luo, Siran Yang, Jingshan Lv, Chi Zhang, Hongbo Deng, et al. 2021. One Model to Serve All: Star Topology Adaptive Recommender for Multi-Domain CTR Prediction. In *Proceedings of the 30th ACM International Conference on Information & Knowledge Management*. 4104–4113.
[20] Hongyan Tang, Junning Liu, Ming Zhao, and Xudong Gong. 2020. Progressive layered extraction (ple): A novel multi-task learning (mtl) model for personalized recommendations. In *Proceedings of 14th ACM Conference on Recommender Systems*. 269–278.
[21] Lisa Torrey and Jude Shavlik. 2010. Transfer learning. In *Handbook of research on machine learning applications and trends: algorithms, methods, and techniques*. IGI global, 242–264.
[22] Xin Wang, Fisher Yu, Lisa Dunlap, Yi-An Ma, Ruth Wang, Azalia Mirhoseini, Trevor Darrell, and Joseph E Gonzalez. 2018. Deep mixture of experts via shallow embedding. *arXiv preprint arXiv:1806.01531* (2018).
[23] Dongbo Xi, Zhen Chen, Peng Yan, Yinger Zhang, Yongchun Zhu, Fuzhen Zhuang, and Yu Chen. 2021. Modeling the Sequential Dependence among Audience Multi-step Conversions with Multi-task Learning in Targeted Display Advertising. *arXiv preprint arXiv:2105.08489* (2021).
[24] Zhuojian Xiao, Yunjiang Jiang, Guoyu Tang, Lin Liu, Sulong Xu, Yun Xiao, and Weipeng Yan. 2021. Adversarial Mixture Of Experts with Category Hierarchy Soft Constraint. In *Proceedings of the IEEE Conference on Data Engineering (ICDE)*. IEEE, 2453–2463.
[25] An Yang, Junyang Lin, Rui Men, Chang Zhou, Le Jiang, Xianyan Jia, Ang Wang, Jie Zhang, Jiamang Wang, Yong Li, et al. 2021. Exploring Sparse Expert Models and Beyond. *arXiv preprint arXiv:2105.15082* (2021).
[26] Yongxin Yang and Timothy M Hospedales. 2014. A unified perspective on multi-domain and multi-task learning. *arXiv preprint arXiv:1412.7489* (2014).
[27] Jiejie Zhao, Bowen Du, Leilei Sun, Fuzhen Zhuang, Weifeng Lv, and Hui Xiong. 2019. Multiple relational attention network for multi-task learning. In *Proceedings of the 25th ACM SIGKDD International Conference on Knowledge Discovery & Data Mining*. 1123–1131.
[28] Ziwei Zhu, Shahin Sefati, Parsa Saadatpanah, and James Caverlee. 2020. Recommendation for new users and new items via randomized training and mixture-of-experts transformation. In *Proceedings of the 43rd International ACM SIGIR Conference on Research and Development in Information Retrieval*. 1121–1130.